

High power ultraviolet light emitting diodes based on GaN/AlGaIn quantum wells produced by molecular beam epitaxy

J. S. Cabalu, A. Bhattacharyya, C. Thomidis, I. Friel, T. D. Moustakas, C. J. Collins, and Ph. Komninou

Citation: *Journal of Applied Physics* **100**, 104506 (2006); doi: 10.1063/1.2388127

View online: <http://dx.doi.org/10.1063/1.2388127>

View Table of Contents: <http://scitation.aip.org/content/aip/journal/jap/100/10?ver=pdfcov>

Published by the [AIP Publishing](#)

Articles you may be interested in

[Ultraviolet light-emitting diodes grown by plasma-assisted molecular beam epitaxy on semipolar GaN \(20°\) substrates](#)

Appl. Phys. Lett. **102**, 111107 (2013); 10.1063/1.4796123

[Quantum-well and localized state emissions in AlInGaN deep ultraviolet light-emitting diodes](#)

Appl. Phys. Lett. **91**, 221906 (2007); 10.1063/1.2817947

[Influence of residual oxygen impurity in quaternary InAlGaIn multiple-quantum-well active layers on emission efficiency of ultraviolet light-emitting diodes on GaN substrates](#)

J. Appl. Phys. **99**, 114509 (2006); 10.1063/1.2200749

[Milliwatt operation of AlGaIn-based single-quantum-well light emitting diode in the ultraviolet region](#)

Appl. Phys. Lett. **78**, 3927 (2001); 10.1063/1.1377854

[GaN/AlGaIn multiple-quantum-well light-emitting diodes grown by molecular beam epitaxy](#)

Appl. Phys. Lett. **74**, 3616 (1999); 10.1063/1.123199



High power ultraviolet light emitting diodes based on GaN/AlGa_N quantum wells produced by molecular beam epitaxy

J. S. Cabalu, A. Bhattacharyya, C. Thomidis, I. Friel, and T. D. Moustakas^{a)}

Department of Electrical and Computer Engineering, Boston University, Boston, Massachusetts 02215 and Center of Photonics Research, Boston University, Boston, Massachusetts 02215

C. J. Collins

U.S. Army Research Laboratory, Adelphi, Maryland 20783

Ph. Komninou

Physics Department, Aristotle University, 54124 Thessaloniki, Greece

(Received 15 February 2006; accepted 8 September 2006; published online 27 November 2006)

In this paper, we report on the growth by molecular beam epitaxy and fabrication of high power nitride-based ultraviolet light emitting diodes emitting in the spectral range between 340 and 350 nm. The devices were grown on (0001) sapphire substrates via plasma-assisted molecular beam epitaxy. The growth of the light emitting diode (LED) structures was preceded by detailed materials studies of the bottom *n*-AlGa_N contact layer, as well as the GaN/AlGa_N multiple quantum well (MQW) active region. Specifically, kinetic conditions were identified for the growth of the thick *n*-AlGa_N films to be both smooth and to have fewer defects at the surface. Transmission-electron microscopy studies on identical GaN/AlGa_N MQWs showed good quality and well-defined interfaces between wells and barriers. Large area mesa devices (800 × 800 μm²) were fabricated and were designed for backside light extraction. The LEDs were flip-chip bonded onto a Si submount for better heat sinking. For devices emitting at 340 nm, the measured differential on-series resistance is 3 Ω with electroluminescence spectrum full width at half maximum of 18 nm. The output power under dc bias saturates at 0.5 mW, while under pulsed operation it saturates at approximately 700 mA to a value of 3 mW, suggesting that thermal heating limits the efficiency of these devices. The output power of the investigated devices was found to be equivalent with those produced by the metal-organic chemical vapor deposition and hydride vapor-phase epitaxy methods. The devices emitting at 350 nm were investigated under dc operation and the output power saturates at 4.5 mW under 200 mA drive current. © 2006 American Institute of Physics. [DOI: 10.1063/1.2388127]

I. INTRODUCTION

Ultraviolet light emitting diodes (UV-LEDs), based on III-nitride semiconductors, are the subject of extensive investigation over the past several years because of their potential for a number of applications. Such applications include biological and chemical identification, water purification, short range communication, solid state lighting, etc. The great majority of the UV-LEDs reported so far in the literature were grown by the metal-organic chemical vapor deposition (MOCVD) method and the active region of these devices consists of Al_xGa_{1-x}N/Al_yGa_{1-y}N multiple quantum wells (MQWs).¹⁻¹⁵ There are limited reports where such LEDs were grown by the hydride vapor-phase epitaxy (HVPE) method¹⁶ or by combining the HVPE and MOCVD methods.¹⁷⁻¹⁹ The molecular beam epitaxy (MBE) method has a number of advantages at this early stage of developing this class of devices. Specifically, the growth can be monitored by reflection high-energy electron diffraction (RHEED) and other *in situ* probes, which are not available for high pressure growth methods. There is only one report of making

UV-LEDs by gas-source MBE using ammonia as the nitrogen source.²⁰

In this paper, we report the growth and fabrication of UV-LEDs, emitting at 340 and 350 nm, by rf plasma-assisted MBE (PAMBE). Contrary to devices made by the MOCVD method, which are based on Al_xGa_{1-x}N/Al_yGa_{1-y}N MQWs, the LEDs of the current work are based on GaN/AlGa_N MQWs. However, in order to obtain 340 nm emission from such devices, the GaN QWs must be very thin. Such devices were found to have a maximum output power of 4.5 mW.

II. EXPERIMENTAL METHODS

The LED structures were grown by rf plasma-assisted molecular beam epitaxy on (0001) sapphire substrates in a Varian Gen II MBE system using an Applied Epi Uni-bulb rf plasma source to activate molecular nitrogen. Ga and Al were supplied from Applied Epi SUMO™ cells and standard effusion cells were used for the evaporation of Mg and Si. Prior to the growth of the device layers, the sapphire surface was converted from Al₂O₃ to AlN by exposing the substrate to nitrogen plasma,^{21,22} followed by the deposition of an AlN buffer layer of approximately 100 nm thick, both done at a

^{a)}Electronic mail: moustakas@bu.edu

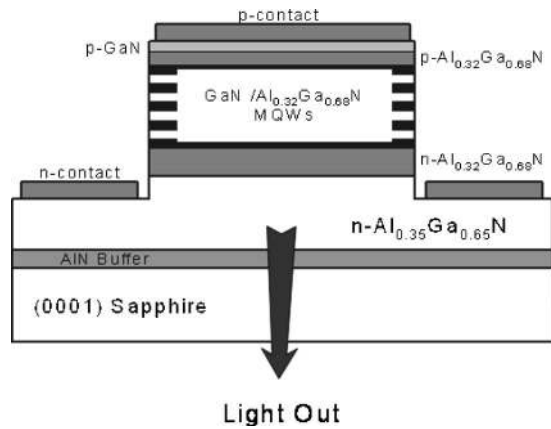


FIG. 1. Schematic illustration of the investigated UV-LED structures showing the various device layers.

substrate temperature of 870 °C. This sequence of nucleation was found to lead to III-nitride materials having the cation polarity.²³

The LED structures were designed for light extraction through the sapphire substrate, by employing a high Al percentage AlGa_n *n*-contact layer compared to the AlGa_n barriers used in the active region of the LED structure, as shown schematically in Fig. 1. The various device layers were grown at a substrate temperature of 770 °C. The bottom Al_{0.35}Ga_{0.65}N layer (2 μm thick) was doped *n* type with silicon to a carrier concentration of 3×10^{19} cm⁻³, followed by 0.4 μm thick Al_{0.32}Ga_{0.68}N doped at the same level. From transmission line measurements (TLMs), we determined that this doping level leads to a sheet resistance of the Al_{0.35}Ga_{0.65}N bottom layer to be 37 Ω/sq.

The active region of the LED structures was based on ultrathin GaN/AlGa_n MQWs. This region consists of five pairs of GaN/Al_{0.32}Ga_{0.68}N MQWs with well and barrier thicknesses of 1 and 2 nm, respectively. During the growth of the quantum wells, we used a certain amount of indium flux to act as a surfactant.²⁴ To determine the internal quantum efficiency of these quantum wells, we have measured their photoluminescence spectra as a function of temperature using a He–Cd laser as an excitation source. Both the *p*-GaN and *p*-Al_{0.32}Ga_{0.68}N layers were deposited using extreme group-III-rich conditions of growth. From our earlier studies, we have shown that under these conditions, Mg incorporation is enhanced and hole concentrations of up to 3×10^{18} cm⁻³ can be achieved.²⁵

The devices were fabricated using standard photolithography and mesas were formed with an inductively coupled plasma (ICP) etching system utilizing pure Cl₂ chemistry. Etching was performed at a chamber pressure of 3.8×10^{-3} Torr, 350 W rf power, and –400 V substrate bias, leading to an etch rate of 100 nm/min. The mesa size of the investigated LED devices is 800×800 μm². After the mesa etching, contacts to the bottom *n*-AlGa_n layer were deposited by e-beam evaporation using Ti (2 nm)/Al (10 nm)/Ti (40 nm)/Au (200 nm) metal scheme followed by rapid thermal annealing (RTA) for 50 s at 850 °C in a nitrogen ambient.^{8,26} Due to relatively poor conductivity of *p*-GaN, as well as *n*-AlGa_n films, III-nitride LED devices suffer from

current crowding effects which lower their device efficiency. Therefore, to facilitate current spreading during the forward biasing of the LED device, almost the entire top of the mesa was coated with the *p*-Ohmic contact metals and the *n* contact was deposited around the periphery of the mesa. Contacts to the *p*-GaN layer, which cover the top of the mesa region of the device, were deposited by e-beam evaporation of Ni (5 nm)/Au (20 nm). These contacts were rapid thermal annealed for 10 min at 500 °C in an oxygen atmosphere. Following the deposition of the Ohmic contacts, thick bond pads for the *n* and *p* contacts were deposited simultaneously by e-beam evaporation using Ni (10 nm)/Au (200 nm). For improvement in the thermal management of the LEDs, individual devices were flip-chip bonded, *p*-side down, onto patterned silicon submounts using either indium bumps or gold stud bumps. These flip-chip bonded devices were mounted on transistor outline (TO-05) headers and gold wires were bonded onto the bond pads to provide electrical connection to the TO leads.

These semipackaged UV-LEDs (without any coating, mirror, or molding) were characterized electrically using an HP4155C semiconductor parameter analyzer and their optical characteristics [electroluminescence (EL) and output power] were measured using a calibrated system which includes an integrating sphere and a calibrated linear array spectrometer.

III. EXPERIMENTAL RESULTS AND DISCUSSION

A. Materials growth studies

In this section, we discuss the growth of the various layers of the LED structure. The bottom AlGa_n thick layer was not deposited directly onto the AlN buffer layer because we have evidence from cross-section transmission-electron microscopy (TEM) studies that under such conditions, re-nucleation takes place leading to a large number of dislocations at the interface. Instead, a graded AlGa_n layer with Al composition varying from 100% to 35% was employed. An important parameter for the growth of AlGa_n films is the ratio of group-III to group-V fluxes. Cross-section TEM studies of bulk AlGa_n films, deposited under different group-III/group-V flux ratios, indicate that under group-III-rich conditions of growth, the threading defects propagate parallel to the growth direction and they do not annihilate.²⁷ Thus, the dislocation density does not reduce with increasing thickness. The surface of the grown film is, however, very smooth, which is ideal for the subsequent deposition of thin MQWs for the active region of the LED. On the other hand, if the films are grown under group-III/group-V ratio close to 1, the dislocations annihilate sharply with increasing film thickness. However, this growth condition leads to a faceted top surface. For this reason, during the growth of the bottom *n*-AlGa_n layer of the LED structures, the majority of the film was deposited under conditions of growth where the group-III/group-V ratio is close to 1 to promote annihilation of threading dislocations, but the final 1000 Å of the film was deposited at excess group-III conditions. This changes the RHEED pattern from slightly spotty to streaky and leads to an atomically smooth surface suitable for the subsequent

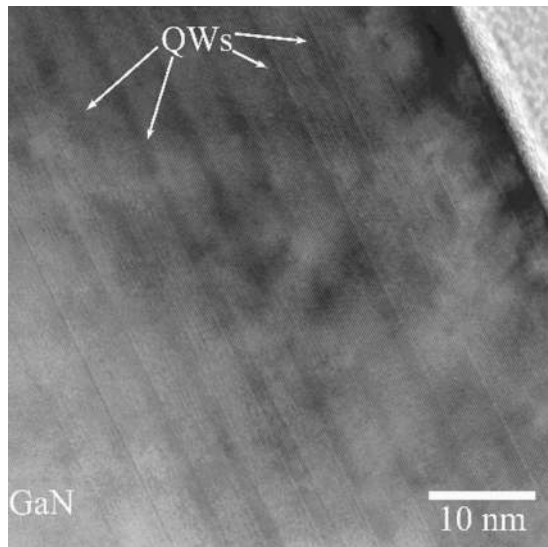


FIG. 2. HRTEM image of GaN/Al_{0.2}Ga_{0.8}N MQWs consisting of barriers having 16 monolayers, and wells having 6 monolayers, viewed along the [1 $\bar{1}$ 00] direction.

growth of the MQWs. Thus, this procedure is expected both to optimize surface microstructure of the film and improve its structural properties by reduction of dislocations.

As discussed earlier, the active region of the LED structures was based on thin GaN quantum wells in order to emit at 340 nm. The choice of using thin GaN quantum wells was further motivated by the fact that the devices were grown along the polar [0001] direction and thin quantum wells mitigate the degrading influence of the polarization effects (quantum confined Stark effect). During the growth of AlGa_xN barriers of the MQW structures, we used additionally a certain amount of indium flux. From our previous studies, we have found that at the growth temperature of 770 °C, indium does not incorporate in the film. However, it was found that the luminescence efficiency of the MQWs increases very significantly compared to those grown without indium flux.²⁴ This methodology of growing GaN/AlGa_xN MQWs was tested by studying the cross-section TEM of MQWs grown under identical conditions as those used in our LED structures. Figure 2 shows high-resolution cross-section TEM image of GaN/Al_{0.2}Ga_{0.8}N MQWs consisting of barriers having 16 monolayers and wells having 6 monolayers viewed along the [1 $\bar{1}$ 00] direction. As seen from these data, good quality and well-defined interfaces are revealed. The internal quantum efficiency at room temperature of these MQWs was calculated by taking the ratio of integrated photoluminescence intensity measured at room temperature and 10 K, and found to be between 30% and 40%.

One difference between the LEDs described in this paper and those produced by the MOCVD method^{1–15} is that we employed GaN/AlGa_xN MQWs with very thin wells (1 nm or four monolayers) while the MOCVD grown devices are based on Al_xGa_{1–x}N/Al_yGa_{1–y}N MQWs with well widths of 2–3 nm. The deposition of such thin wells is possible because growth during MBE can be controlled with atomic layer precision.

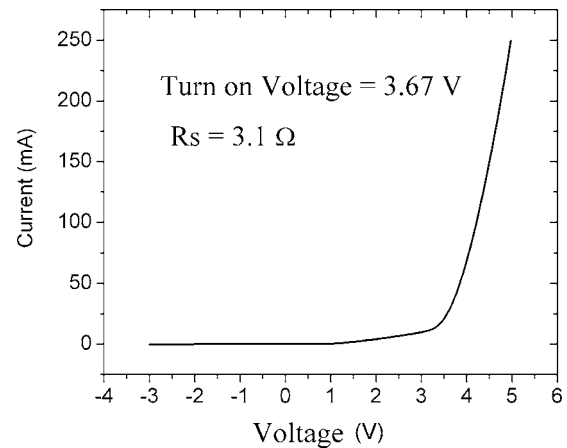


FIG. 3. *I*-*V* characteristics of an UV-LED device emitting at 340 nm. Indicated in the inset of the figure are the turn-on voltage and on-series resistance of the device.

B. LED devices emitting at 340 nm

The *I*-*V* characteristics of a LED device with mesa dimensions of 800 × 800 μm² are shown in Fig. 3. This device exhibits a rectifying behavior and has a sharp turn-on voltage at approximately 3.7 V. The typical differential on-series resistance R_s for many of the devices tested is only 3 Ω, which is significantly smaller than the values reported in the literature for UV-LEDs emitting at the same wavelength.^{3,18} A low on-series resistance suggests that the bottom *n*-AlGa_xN layer has good electrical properties since R_s depends largely on the conductivity of the *n*-contact layer.²⁸

The electroluminescence spectra of one of the tested devices, plotted in output power/nanometer versus wavelength, were investigated both under dc and ac drive currents. Under dc drive current [Fig. 4(a)], the spectra were investigated only up to 280 mA, where the output power starts to saturate due to device heating. Under ac drive current [Fig. 4(b)], the device was investigated up to 700 mA. To mitigate device self-heating, we used 100 μs long current pulses with a repetition frequency of 1 kHz. In both cases, the full width at half maximum (FWHM) is between 18 and 19 nm. There is an observed small blueshift in the peak of the EL spectra from 343 to 341 nm with the increase of the drive current. This blueshift in the peak is qualitatively consistent with band filling. It is important to note that there are no subband gap transitions, which are related to carrier recombination at deep levels in the active region. The same result also suggests that the design of the electron blocking layer was good enough to prevent recombination in the *p*-GaN layer. This is to be contrasted with earlier works on similar LEDs grown by other methods.^{3,16}

The integrated output power versus drive current for both dc and pulsed operations is shown in Fig. 5. It is apparent from these data that under dc drive current, the output power begins to saturate due to heating at about 0.5 mW under 200 mA drive current which translates to a wall-plug efficiency of 0.053%. On the contrary, under pulsed drive current, the output power saturates at about 2.75 mW under 700 mA drive current. The difference between the dc and pulsed operations suggests that, although the UV-LED de-

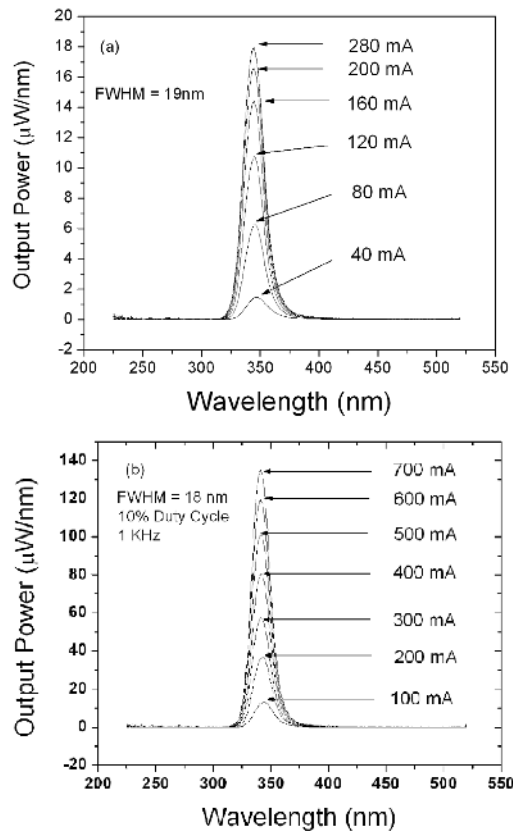


FIG. 4. Electroluminescence spectra, plotted as output power/nanometer vs wavelength, of an UV-LED device with a peak intensity at 340 nm under (a) dc and (b) pulsed operations at various drive currents.

vices have been flip-chipped onto Si submounts, they still suffer from heat degradation. Studies show that a better flip-chip package design and a better choice of submount with higher thermal conductivity are needed to more efficiently transfer heat away from the junction.²⁹

C. LED devices emitting at 350 nm

UV-LEDs with peak wavelengths at 350 nm and with similar mesa dimensions as the ones emitting at 340 nm were evaluated under dc drive current up to 200 mA. Figure

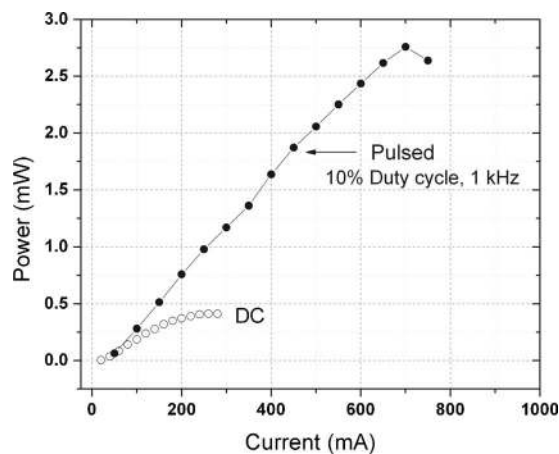


FIG. 5. Integrated power output of an UV-LED device with a peak intensity at 340 nm under dc and pulsed operations vs drive current.

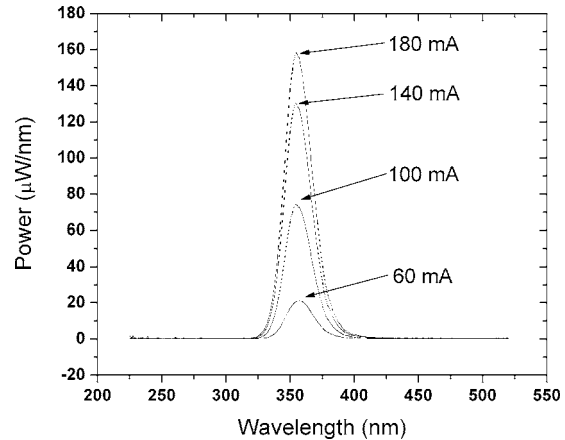


FIG. 6. Electroluminescence spectra, plotted as output power/nanometer vs wavelength, of an UV-LED device with a peak intensity at 350 nm under dc operation at various drive currents.

6 shows the EL spectra plotted as output power/nanometer versus wavelength. The spectra have a FWHM of 25 nm and there are no deep level emissions. Figure 7 shows the integrated output power versus drive current for the device discussed in Fig. 6. As seen from these data, the maximum output power is 4.5 mW under a drive current of 200 mA, which translates to a wall-plug efficiency of 0.24%. At this drive current, the output power begins to saturate due to device heating. Nishida *et al.*¹⁰ also reported UV-LEDs emitting at 350 nm grown by low-pressure metal-organic vapor-phase epitaxy (LP-MOVPE). These authors reported a maximum output power of 7 mW at 220 mA under dc operation. However, they did not report the size of their device and thus we are unable to make direct comparison with our data.

It is difficult to compare the performance of our UV-LEDs with those reported in the literature and grown by the MOCVD (Ref. 30) and HVPE (Ref. 16) methods, because the reported data were taken on devices of different sizes and thus, issues of edge versus surface emission as well as heat transfer to heat sink differ from device to device. An elementary comparison of our data with those reported in the literature is in presented Table I. These data indicate that all three methods produce practically equivalent devices.

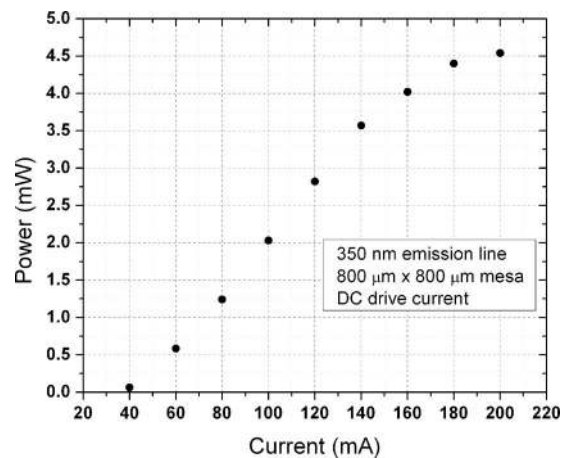


FIG. 7. Integrated power output of an UV-LED device with a peak intensity at 350 nm under dc operation vs drive current.

TABLE I. Comparison of UV-LEDs emitting in the spectral region of 340–350 nm and produced by MOCVD, HVPE, and MBE (current work).

Growth method	Device size	Peak wavelength	Driving current	Optical output	Ref.
MOCVD	200 × 200 μm^2 four devices connected in parallel	340 nm	1000 mA (pulsed)	13 mW	30
HVPE	330 × 330 μm^2	341 nm	110 mA	2.3	16
MBE	800 × 800 μm^2	340 nm	700 mA (pulsed)	2.75 mW	Current work
	800 × 800 μm^2	350 nm	200 mA (cw)	4.5 mW	

IV. CONCLUSIONS

In conclusion we reported the growth by plasma-assisted MBE and fabrication of UV-LEDs emitting in the spectral region of 340–350 nm. Kinetic conditions were identified for the growth of the thick *n*-AlGaIn to be both smooth and to have fewer defects at the interface. Specifically, we found that under group-III-rich conditions, the Si-doped AlGaIn films have smooth surfaces. However, under those conditions, the dislocations propagate parallel to the growth direction and they do not annihilate as a function of film thickness. On the other hand, under growth conditions of group III/group V equal to 1, the dislocations tend to annihilate as the film grows thicker. However, such conditions lead faceted surfaces. Thus during the growth of the bottom *n*-AlGaIn contact layer, a combination of these two conditions was used to produce smooth films with fewer defects at the surface. These devices employ five GaN/Al_{0.32}Ga_{0.68}N MQWs with narrow wells (~1 nm) as the active region of the device. TEM cross-section studies of a similarly grown MQWs consisting of barriers having 16 monolayers and wells having 6 monolayers show good quality and abrupt interfaces between the wells and the barriers. Devices with mesa dimensions of 800 × 800 μm^2 were flip-chip bonded onto silicon submounts and were evaluated under both dc and pulsed drive currents. Under dc operation the output power of the 340 nm devices was found to saturate at about 200 mA to a level of 0.5 mW. Under pulsed operation the peak output power of the devices does saturate at about 700 mA to a level of 2.75 mW. These results suggest that a better choice of submount with higher thermal conductivity is needed to more efficiently transfer heat away from the junction. By comparing the output power for UV-LEDs emitting at 340 nm and grown by the MOCVD, HVPE, and MBE methods we found that the reported devices have practically a similar performance independent of the method of growth. Devices with the same dimensions emitting at 350 nm were evaluated only under dc drive current and found to have an output power of 4.5 mW under dc drive current of 200 mA, translating to a wall-plug efficiency of 0.24%. These results are currently the best ever reported in literature for UV-LEDs grown by PAMBE.

ACKNOWLEDGMENTS

This work was supported by DARPA under the program SUVOS, by DOE under the Solid State Lighting Program

and by CUNY under the Compact Photonics Explorer's Consortium. The authors would also like to thank Dr. Phil Lamarre and Dr. William Stacey of Photronix, Inc., and Dan Pascual of Suss Microtech, Inc., for their help and advice with regard to device fabrication and flip-chip bonding.

- ¹J. Han *et al.*, Appl. Phys. Lett. **73**, 1688 (1998).
- ²A. Kinoshita, H. Hirayama, M. Ainoya, Y. Aoyagi, and A. Hirata, Appl. Phys. Lett. **77**, 175 (2000).
- ³V. Adivarahan *et al.*, Appl. Phys. Lett. **79**, 4240 (2001).
- ⁴T. Wang, Y. H. Liu, Y. B. Lee, J. P. Ao, J. Bai, and S. Sakai, Appl. Phys. Lett. **81**, 2508 (2002).
- ⁵H. Hirayama, A. Kinoshita, T. Yamabi, Y. Enomoto, A. Hirata, T. Araki, Y. Nanishi, and Y. Aoyagi, Appl. Phys. Lett. **80**, 207 (2002).
- ⁶A. Chitnis *et al.*, Appl. Phys. Lett. **81**, 2938 (2002).
- ⁷A. Chitnis *et al.*, Appl. Phys. Lett. **81**, 3491 (2002).
- ⁸V. Adivarahan *et al.*, Appl. Phys. Lett. **81**, 3666 (2002).
- ⁹J. P. Zhang *et al.*, Appl. Phys. Lett. **81**, 4910 (2002).
- ¹⁰T. Nishida, N. Kobayashi, and T. Ban, Appl. Phys. Lett. **82**, 1 (2003).
- ¹¹A. Chitnis, J. P. Zhang, V. Adivarahan, M. Shatalov, S. Wu, R. Pachipulusu, V. Mandavilli, and M. A. Khan, Appl. Phys. Lett. **82**, 2565 (2003).
- ¹²J. P. Zhang, S. Wu, S. Rai, V. Mandavilli, V. Adivarahan, A. Chitnis, M. Shatalov, and M. A. Khan, Appl. Phys. Lett. **83**, 3456 (2003).
- ¹³A. J. Fischer *et al.*, Appl. Phys. Lett. **84**, 3394 (2004).
- ¹⁴V. Adivarahan *et al.*, Appl. Phys. Lett. **85**, 1838 (2004).
- ¹⁵V. Adivarahan, W. H. Sun, A. Chitnis, M. Shatalov, S. Wu, H. P. Maruska, and M. A. Khan, Appl. Phys. Lett. **85**, 2175 (2004).
- ¹⁶G. A. Smith, T. N. Dang, T. R. Nelson, J. L. Brown, D. Tsvetkov, A. Usikov, and V. Dmitriev, J. Appl. Phys. **95**, 8247 (2004).
- ¹⁷T. Nishida, H. Saito, and N. Kobayashi, Appl. Phys. Lett. **79**, 711 (2001).
- ¹⁸A. Yasan *et al.*, Appl. Phys. Lett. **81**, 2151 (2002).
- ¹⁹A. Yasan, R. McClintock, K. Mayes, S. R. Darvish, P. Kung, M. Razeghi, and R. J. Molnar, Opto-Electron. Rev. **10**, 287 (2002).
- ²⁰G. Kipshidze, V. Kuryatkov, B. Borisov, M. Holtz, S. Nikishin, and H. Temkin, Appl. Phys. Lett. **80**, 3682 (2002).
- ²¹T. D. Moustakas, R. J. Molnar, T. Lei, J. Menon, and C. R. Eddy, Jr., Mater. Res. Soc. Symp. Proc. **242**, 427 (1992).
- ²²T. D. Moustakas, T. Lei, and R. J. Molnar, Physica B **185**, 36 (1993).
- ²³T. D. Moustakas, E. Iliopoulos, A. V. Sampath, H. M. Ng, D. Doppalapudi, M. Misra, D. Korakakis, and R. Singh, J. Cryst. Growth **227/228**, 13 (2001).
- ²⁴A. Bhattacharyya *et al.*, J. Cryst. Growth **251**, 487 (2003).
- ²⁵A. Bhattacharyya, W. Li, J. Cabalu, T. D. Moustakas, D. J. Smith, and R. L. Hervig, Appl. Phys. Lett. **85**, 4956 (2004).
- ²⁶D. F. Wang, F. Shiwei, C. Lu, A. Motayed, M. Jah, S. N. Mohammad, K. A. Jones, and L. S. Riba, J. Appl. Phys. **89**, 6214 (2001).
- ²⁷L. T. Romano, B. S. Krusor, R. Singh, and T. D. Moustakas, J. Electron. Mater. **26**, 285 (1997).
- ²⁸I. Eliashevich, Y. Li, A. Osinski, C. A. Tran, M. G. Brown, and R. F. Karliceck, Jr., Proc. SPIE **3621**, 28 (1999).
- ²⁹M. Shatalov *et al.*, Appl. Phys. Lett. **86**, 201109 (2005).
- ³⁰M. A. Khan, Proc. SPIE **4996**, 188 (2003).